ACADEMIA ROMÂNĂ
Revue Roumaine de Chimie
http://web.icf.ro/rrch/

Rev. Roum. Chim.,
2016, *61*(2), 125-130

SYNTHESIS AND CHARACTERIZATION OF GOLD NANOPARTICLES FUNCTIONALIZED WITH CALAMITIC MESOGENS

Liliana CSEH[a,b,*] and Georg H. MEHL[b]

[a] Institute of Chemistry Timişoara of the Roumanian Academy, 24 Mihai Viteazul Bv., RO-300223 Timişoara, Roumania
[b] University of Hull, Chemistry Department, Cottingham Road, HU6 7RX, Hull, UK

Received November 17, 2015

Liquid-crystalline nanoparticles represent an exciting class of new materials for a variety of potential applications. By combining supramolecular ordering with the fluid properties of the liquid-crystalline state, these materials offer the possibility to organize nanoparticles into addressable 2-D and 3-D arrangements exhibiting high processability and self-healing properties.
Here, we report the influence of temperature or/and ratio of reactants (C_6H_5-SH and $HAuCl_4$) on the size of gold nanoparticles (**NH**). The synthesis of gold nanoparticles which are covered with thermotropic liquid crystals (4'-(undecyloxy)biphenyl-4-yl 4-(11-mercapto-undecyloxy)benzoate) (**L**) – rod like mesogen by ligand exchange reaction it is also presented. The nanoparticles are functionalized with two different thiol molecules: simple n-hexane thiol and rod like mesogen.
Chemical structures and purity of nanoparticles were confirmed by ^{1}H-NMR and elemental analysis. The size of spherical particles were estabilised by TEM. The hybrid gold nanoparticles (**NHL**) show mesophase behavior in a large temperature interval above 43ºC and the nanocomposites are stable up to 145ºC.

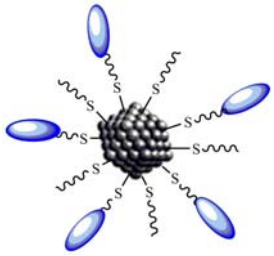

INTRODUCTION

Gold nanoparticles (NPs) are of the great interest for electronic,[1] optic[2] and photonic applications.[3] The adding of colloidal particles to liquid crystals has been largely based on their ability by significantly alter the dielectric behaviour of liquid crystals (LC), which could potentially result in faster switching devices.[4-8] The most common method for inducing LC phases in NP hybrids is to introduce a suitable LC ligand onto the surface of the nanoparticle. In this way, it is expected that the mesogenic properties of the ligand will be transferred to the hybrid product. Until now, only few hybrid nanoparticles with liquid crystal properties have been reported. For example, In *et al.*[9] described the end-attaching cyanobiphenyl mesogens to gold nanoparticles via a thioalkyl spacer. The authors observed a nematic phase in which the particles formed wormlike chains. A number of ligands of end-on chain type were reported by Gorecka *et al.*, where the mesogens were grafted on gold nanoparticles to induce smectic and columnar phases.[10, 11] Nanoparticles covered by rod-like mesogens attached laterally via a thioalkyl[12-15] or aminoalkyl[16] spacer were found to give nematic phase of the mesogens, though for small particles 2D and 3D superstructures of NPs were found[17] and this was recently extended to chiral materials.[18] Bent core derivatives grafted on gold nanoparticles were found to form a metastable LC phase of unknown nature.[19] A number of mesomorphic dendritic LC ligands have been used[20,21] for the functionalization of NPs. The mesomorphic properties of ligands usually failed to give their mesomorphism to the NPs system, though interestingly, when they were deposited on surfaces, organization in layer-like structures was detected. Two dendrons are known, reported by Deschenaux *et al.*,[22] inducing smectic A phase. The first simple-cubic liquid crystal was obtained by coating monodisperse Au nanoparticles (NPs) with a thick corona of amino-substituted organic dendrons by Goran *et al.*[23,24]

Based on the results highlighted above and our experience in the design of liquid crystals gold

* Corresponding author: lili_cseh@yahoo.com; tel.: 0256-491818; fax: 0256-491824

nanoparticles, we conclude that: 1) the presence of two type of ligands attached on the gold core, one hydrocarbon chain and other mesogenic type, ensures avoiding congestion around the core and thus favoring the mesomorphic properties of hybrid nanoparticles and, 2) all of the chosen ligands to promote mesopases in hybrid NPs, have: *(i)* a flexible spacer between the rigid rod-like segment of the molecule; *(ii)* the functional group used to attach the ligand to the NP surface and, *(iii)* in the case of pseudo-spherical NPs, the ligands usually display sizes commensurate with the size of the inorganic bulk.

Liquid crystalline gold nanoparticles (LCNPs) represent interesting materials for the development of nanotechnology by the "bottom-up" approach.[25] The investigation of LCNPs requires the preparation of compounds with specific design and a large variety of mesophases. This goal can be reached only by synthesis of new LCNPs.

Here, we report the synthesis and characterization of new gold nanoparticles covered with hexanethiol (**H)**, as hydrocarbon units, and 4'-(undecyloxy)biphenyl-4-yl-4-(11-mercapto-undecyloxy)benzoate (**L**), as mesogenic units.

RESULTS AND DISCUSSION

Synthesis of gold nanoparticles **NHa-d** covered with hexanethiol was carried out in order to establish the optimum parameters (Table 2). It was found that the diameter of gold nanoparticles decreases by increasing the ratio of hexanthiol/$HAuCl_4$ and decreasing the reaction temperature in the reduction step of the synthesis of gold nanoparticles. Based on these results, the particles of the **NHd** type were chosen to be used in the next step, the functionalization of nanoparticles. This selection was done taking into consideration the size of gold core and the number of ligands attached to the surface. The aim was to avoid congestion around the core and thus favoring the mesomorphic properties of hybrid LC nanocomposites.

The purity of nanoparticles **NH** and **NHL** was verified by ^{1}H-NMR. The ^{1}H-NMR spectra (Fig. 1) demonstrate that thiols are strongly chemisorbed to the gold cores and are not present as free surfactant thiols. The spectra of nanoparticles are broadened when compared to those of the free thiols and the peak at 2.51 ppm, correspondig to the proton in the α position to the -SH (-C**H**$_2$-SH) of **L**, disappears (Fig. 1b).

The strong broadening of the proton signals from **NH** and **NHL** can occur due to a large spin-spin relaxation and a densely packed of the end bulk chain, only for **NHL**. [26]

The number of organic groups covering the surface of the nanoparticles was calculated by combination of elemental analysis, ^{1}H-NMR and TEM. The diameter of nanoparticles was determined by transmission electron microscopy (TEM) (see the details shown in Fig. 2). The dimension of the nanoparticles was determined to be 1.6 ± 0.4 nm. The number of gold atoms/particle was calculated using the following formula[26, 27]: $N_{Au} = 4 * \pi * R^3 / (3 * \nu_g)$; where: R – radius of nanoparticle (Å); D – diameter of nanoparticle (Å); ν_g – volume of a gold atom (ν_g = 17 Å^3). It is assumed that all nanoparticles have a spherical shape. Based on the calculation it was estimated that each particle contains about 140 gold atoms/particle. The gold core size was kept constant after the interchange reaction.

The number of ligands grafted on one nanoparticle (n_s) was calculated using the formula[26]: $n_s = N_{Au} / X$, where X was taken from the elemental analyis as the atomic ratio Au / S = X.

The ^{1}H-NMR spectra of **NH** and **NHL** were used to calculate the ratio of hexanethiol to mesogens **L** attached to a particle by using the ratios of the corresponding peak integrals. Based on this, the ratio of hexanethiol: **L** was found to be 1:1.

Table 1

Characteristics of the **NHa-d** nanoparticles

	hexanethiol/ $HAuCl_4$	Temperature [°C]	Diameter of **NH** (nm)	Number of gold atoms/particle	Number of hexanethiol ligands/particle
NHa	1.5	r.t.	2.1 ± 0.4	285	91
NHb	2	r.t.	1.7 ± 0.4	165	88
NHc	2	0	1.7 ± 0.3	151	78
NHd	3	0	1.6 ± 0.3	140	60

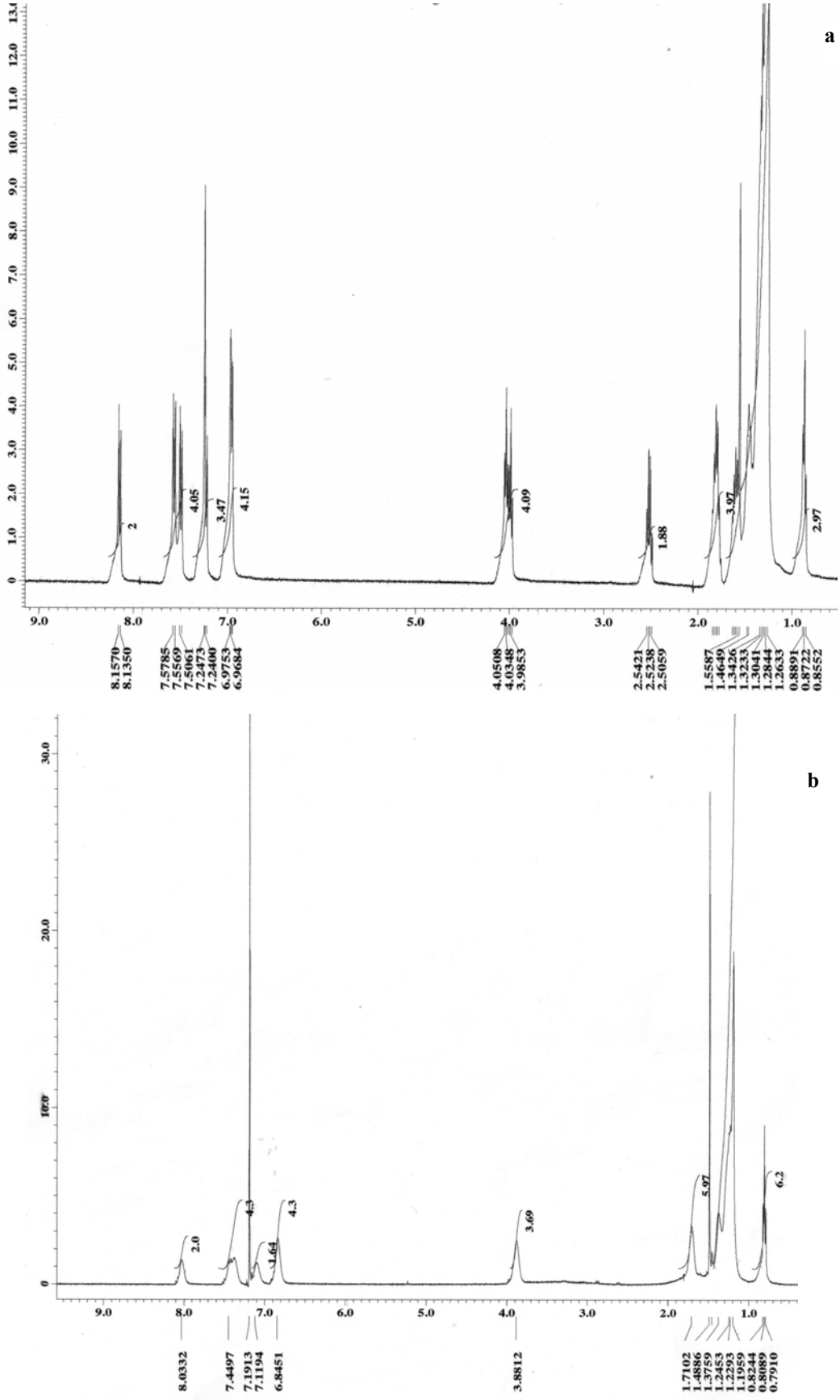

Fig. 1 – ^{1}H-NMR spectra of: a) **L** and b) gold nanoparticles **NHL**.

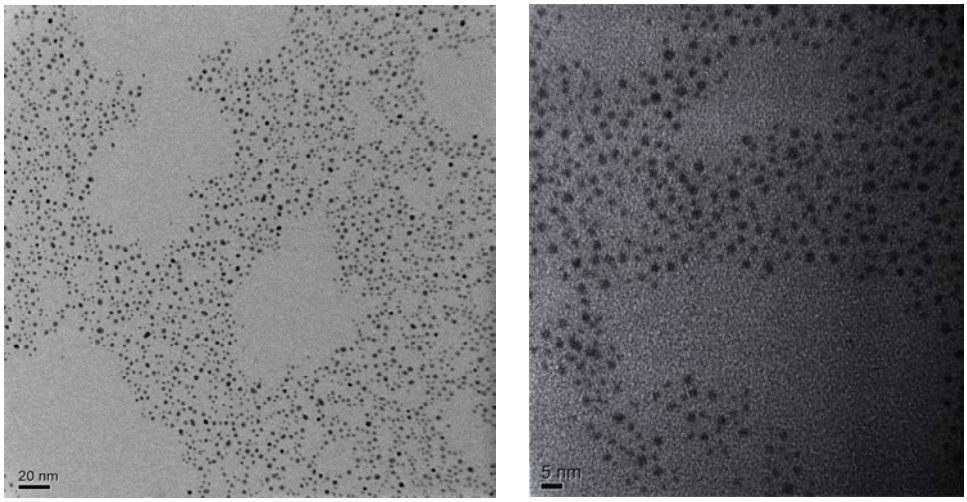

a) b)

Fig. 2 – TEM picture on a graphite surface of: a) **NHd** – Scale bar for picture is 20 nm; and b) **NHL –** Scale bar for picture is 5 nm.

Table 2

Transition temperatures determined by DSC on the secod heating and cooling scans

Compound	**Transition temperatures/°C (Enthalpy/J*g^{-1})**
L	Cr I 95.3(74.5) CrII 117.8 (7.9) SmC 142.0 SmA[a] 160.9 (2.5) N 166.1(2.1) Iso Iso165.5 (2.5) N 160.5 (2.2) SmA [a] 141 SmC117.0 (7.4) CrI 74.7 (22.8) CrII
NHL	Cr 43.5 (1.7) X mesophase 132.5 (0.5) Iso Iso 120.7 (0.8) X mesophase

a – transition found by OPM

The thermal transitions of ligand[28] and functionalised nanoparticles were determined by differential scanning calorimetry (DSC) and are presented in Table 2.

The DSC trace of NH**L** shows on heating, two broad peaks. The first peak at 43.5°C was associated with the crystalline to mesophase transition, while the second peak at 132.5°C was attributed with the transition from the mesophase to an isotropic state. Heating the sample above 145°C showed that the material started to degrade, likely by delamination of the ligand form the particles with the formation of free ligands, see Fig. 3a.

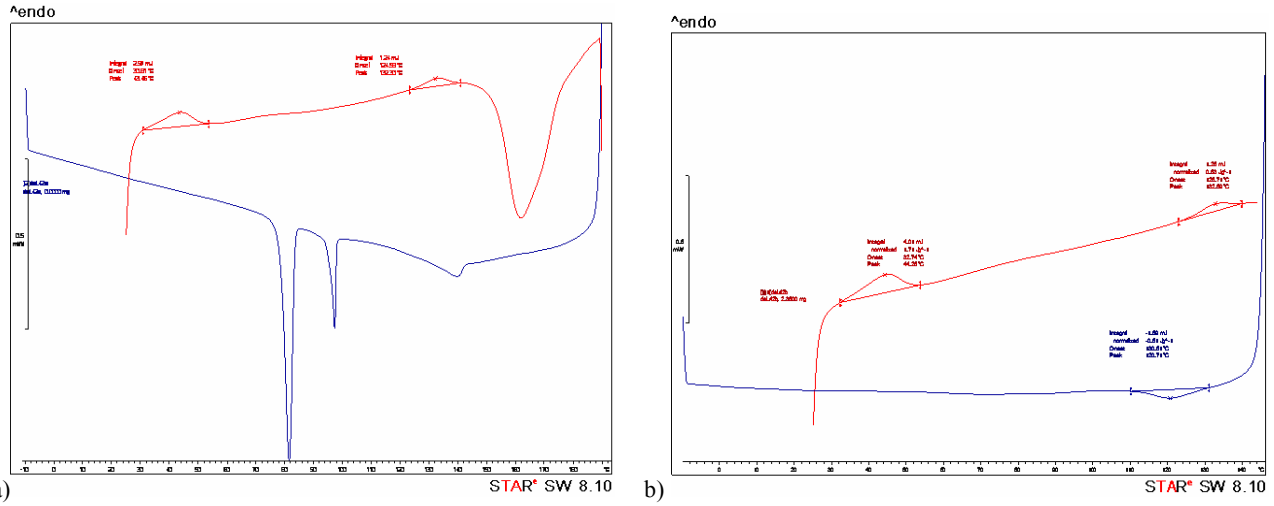

a) b)

Fig. 3 – DSC thermograms of **NHL**: a) on heating-cooling cycle in the temperature range of 25°C ÷ 190°C ÷ -10°C; b) on heating-cooling second cycle in the temperature range of 25°C ÷ 145°C ÷ -10°C.

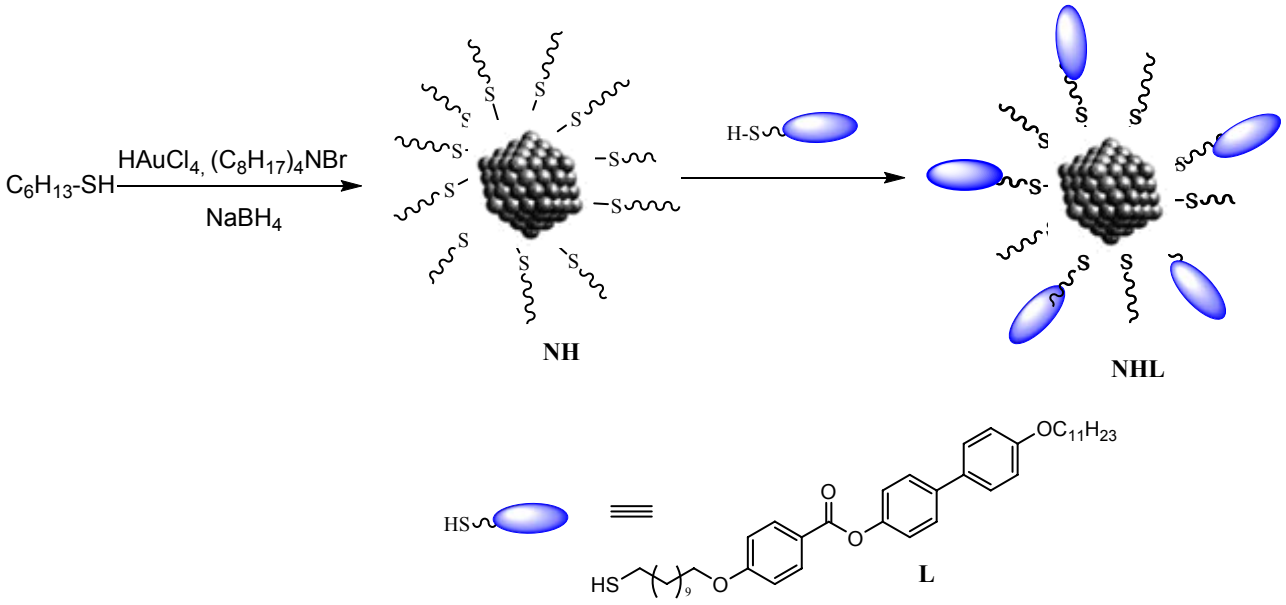

Scheme 1 – Synthesis of gold nanoparticles.

In order to determine the formation of mesophase more clearly, a new sample was prepared and a new thermograme of **NHL** was recorded (Fig. 3b). The sample was heated only up to 145 °C, below the temperature of decomposition. The bahaviour of materials on cooling, second cicle, shows one peak associated to the isotropic to mesophase transition at 120.7°C. The enthalpy values for the **NHL** are relatively low, but comparable to those observed for similar systems.[12, 13]

Viewing NHL at temperatures where the mesomorphic state was detected by the DSC experiments under a polarizing microscope did not show birefringent textures. Such behaviour has been observed before for linear mesogens[10] as well as for mesogens connected laterally to the NPs.[15] It can be associated with the high viscosity of the system, or packing constraints of the mesogens positioned between the nanoparticles which can form complex superstructures. The investigation of the structure of the NHL superlattices is the subject of current investigations.

EXPERIMENTAL

1. Measurements: Nuclear magnetic resonance (NMR) spectra were taken on a Jeol JNM-ECP 400 MHz FT-NMR spectrometer and chemical shifts are reported in ppm relative to TMS. Analytical data were obtained by a Perkin Elmer model 240C elemental analyzer. The thermal properties were investigated using a Mettler Toledo differential calorimeter (DSC) 822e **822e** in nitrogen. The instrument was calibrated with indium. Transition temperatures were determined as the onset of the maximum in the endotherm or exotherm procces. The mesophases were studied on an Olympus BH-2 optical polarising microscope (OPM), equipped with a Mettler FP82 HT hot stage and a Mettler FP90 central processor. Transmission electron micrographs were recorded with a JEOL JEM 3010 Transmission Electron Microscope (point resolution 0.17 nm) equipped with a GATAN GIF 200 electron imaging filter.

2. Chemical synthesis: All the reagents and solvents were purchased (from Merck, Aldrich, Avocado, Fluka sau Lancaster) and used without further purification.

The synthesis and characterization of 4'-(undecyloxy)biphenyl-4-yl 4-(11-mercapto-undecyloxy)benzoate (**L**) was reported[28] and the monolayer-protected clusters (**NH**) (Scheme 1) with hexanethiolate monolayers were prepared following the Schiffrin-Brust method.[29] The **NHa-d** were obtained by changing the temperature or/and ratio of reactants (C_6H_5-SH and $HAuCl_4$) - (Table 1). The purification of **NHa-d** was realised by recristalization from etanol and acetonitrile.

NHa:EA: Found: C 9.39%, H 1.85%, S 4.49%, Au 83.97%; Atomic ratio: Au/S = X = 3.13;
^{1}H-NMR 400 MHz, C_6D_6/δ [ppm]: 1.28 (-CH_2-); 0.84 (-CH_3);
TEM: D = 2.1 ± 0.4 nm;
No. Au atoms/particle = N_{Au} = 285; No. hexanethiol/particle = n_s = 91.

NHb:EA : Found: C 14.96%, H 2.68%, S 6.85%, Au 76.07%; Atomic ratio: Au/S = X = 1.86;
^{1}H-NMR 400 MHz, C_6D_6/δ [ppm]: 1.26 (-CH_2-); 0.84 (-CH_3);
TEM: D = 1.7 ± 0.4 nm;
No. Au atoms/particle = N_{Au} = 165; No. hexanethiol/particle = n_s = 88.

NHc: EA Found: C 15.53%, H 2.62%, S 6.33%, Au 73.97%; Atomic ratio: Au/S = X = 1.94;
^{1}H-NMR 400 MHz, C_6D_6/δ [ppm]: 1.28 (-CH_2-); 0.86 (-CH_3);
TEM: D = 1.7 ± 0.3 nm;
No. Au atoms/particle = N_{Au} = 151; No. hexanethiol/particle = n_s = 78.

NHd:EA : Found: C 12.56%, H 2.30%, S 5.63%, Au 8015%; Atomic ratio: Au/S = X = 2.30;

^{1}H-NMR 400 MHz, C_6D_6/δ [ppm]: 1,26 (-CH_2-); 0,85 (-CH_3); **TEM:** D = 1.6 ± 0.3 nm;
No. Au atoms/particle = N_{Au} = 140; No. hexanethiol/particle = n_s = 60.
Functionalization of **NH** was effected by exchange reactions of hexanethiol with ligand **L.** A solution of **L** (0.47 g, 0.71 mmol) in CH_2Cl_2 (30 ml) was added under sttiring and inert gas to a solution of **NHd** (0.23 g) and CH_2Cl_2 (35 ml) at room temperature. After 61 h, the solvent was removed under reduced pressure. The mixed nanoparticles **NHL** were purified on Bio-Beads S-X1 column, using CH_2Cl_2 as eluant. The black solid was dried under vacuum. **NHL** are air-stable and soluble in chloroform, toluene, dichloromethane, benzene, and other nonpolar solvents.
EA: Found: C 35.09%, H 4.03%, S 3.58%, Au 54.64%; Atomic ratio: Au/S = X= 2.31;
^{1}H-NMR 400 MHz, $CDCl_3$/δ [ppm]: 8.03 ($H_{ar,}$ 2H); 7.44 ($H_{ar,}$ 4H); 7.12 ($H_{ar,}$ 2H); 6.84 ($H_{ar,}$ 4H); 3.88 (-O-CH_2-, 4H); 1.71 (-CH_2-, 6H); 1.23 (-CH_2-); 0.81 (-CH_3, 6H); **TEM**: D = 1.6 ± 0.3 nm; No. Au atoms/particle = N_{Au} = 140; No. of thiols/particle = n_s = 60 ± 5; mesogens/particle 30 ÷ 32.

CONCLUSIONS

We have prepared novel liquid crystal gold nanoparticles, where the spherical particles are covered with a monolayer of hydrocarbon chains and calamitic mesogens. The hybrid gold nanoparticles **NHL** show mesophase behavior in a large temperature interval above 43ºC and the nanocomposites are stable up to 145ºC. The superstructure of the NPs in the organized organic matrix needs to be explored further in the detailed XRD investigations.

Acknowledgments: L.C. thanks the EU for funding through the project "DesignLC" (HPMT-CT2001-00322).

REFERENCES

1. S. W. Boettcher, N. C. Strandwitz, M. Schierhorn, N. Lock, M. C. Lonergan and G. D. Stucky, *Nat. Mater*., **2007**, *6*, 592.
2. E. Ouskova, D. Lysenko, S. Ksondzyk, L. Cseh, G.H. Mehl, V. Reshetnyak and Y. Reznikov, *Mol. Cryst. Liq. Cryst.*, **2011**, *545*, 1347.
3. P. N. Prasad, "Nanophotonics*"*, Wiley, Hoboken, NJ, **2004**.
4. H. Yoshikawa, K. Maeda, Y. Shiraishi, J. Xu, H. Shiraki, N. Toshima and S. Kobayashi, *Jpn. J. Appl. Phys. Part 2*, **2002**, *41*, L1315.
5. Y. Reznikov, O. Buchnev, O. Tereshchenko, V. Reshetnyak and A. Glushchenko, J. West, *Appl. Phys. Lett*., **2003**, *82*, 1917.
6. F. Li, O. Buchnev, C. I. Cheon, A. Glushchenko, V. Reshetnyak, Y. Reznikov, T. J. Sluckin and J. L. West, *Phys. Rev. Lett*., **2006**, *97*, 147801.
7. H. Qi and T. Hegmann, *J. Mater. Chem*., **2006**, *16*, 4197.
8. H. Qi and T. Hegmann, *J. Mater. Chem*., **2008**, *18*, 3288.
9. I. In, Y.-W. Jun, Y. J. Kim and S. Y. Kim, *Chem. Commun.*, **2005**, 800-801.
10. M. Wojcik, W. Lewandowski, J. Matraszek, J. Mieczkowski, J. Borysiuk, D. Pociecha and E. Gorecka, *Angew. Chem.*, *Int. Ed.*, **2009**, *48*, 5167-5169.
11. M. Wojcik, M. Kolpaczynska, D. Pociecha, J. Mieczkowski and E. Gorecka, *Soft Matter*, **2010**, *6*, 5397-5400.
12. L. Cseh and G. H. Mehl, *J. Am. Chem. Soc.*, **2006**, *128*, 13376-13377.
13. L. Cseh and G. H. Mehl, *J. Mater. Chem.*, **2007**, *17*, 311-315.
14. X. Zeng, F. Liu, A. G. Fowler, G. Ungar, L. Cseh, G. H. Mehl and J. E. Macdonald, *Adv. Mater*., **2009**, *21*, 1746.
15. X. Mang, X. Zeng, B. Tang, F. Liu, G. Ungar, R. Zhang, L. Cseh and G. H. Mehl, *J. Mater. Chem.* **2012**, *22*, 11101.
16. C.H. Yu, C. Schubert, B. J. Tang, C. Welch, M.G. Tamba and G. H. Mehl, *J. Am. Chem. Soc.* **2012**, *134*, 5076-5079.
17. J. Dintinger, B. J. Tang, X. Zeng, F. Liu, T. Kienzler, G. H. Mehl, G. Ungar, C. Rockstuhl and T. Scharf, *Adv. Mater.*, **2013**, *25*, 1999-2004.
18. L. Cseh, X. Mang, X. Zeng, F. Liu, G. H. Mehl, G. Ungar and G. Siligardi, *J. Am. Chem. Soc.*, **2015**, *137*, 12736-12739.
19. V. M. Marx, H. Girgis, P. A. Heiney and T. Hegmann, *J. Mater. Chem*., **2008**, *18*, 2983.
20. B. Donnio, P. García-Vázquez, J-L. Gallani, D. Guillon and E. Terazzi, *Adv. Mater.*, **2007**, *19*, 3534-3539.
21. S. Freina, J. Boudonb, M. Vonlanthena, T. Scharfc, J. Barbera, G. Süss-Finka, T. Bürgi and R. Deschenaux, *Helvetica Chim. Acta*, **2008**, *91*, 2321-2337.
22. S. Mishler, S. Guerra and R. Deschenaux, *Chem. Commun*., **2012**, *48*, 2183-2185.
23. M. Matsubara, A. Miyazaki, X. Zeng, A. Maramatsu, G. Ungar and K. Kanie, *Molec. Cryst. Liq. Cryst*., 2015, *617*, 50-57.
24. K. Kanie, M. Matsubara, X. Zeng, F. Liu, G. Ungar, H. Nakamura and A Muramatsu, *J. Amer. Chem Soc.*, **2012**, *134*, 808-811.
25. M. Draper, I. M. Saez, S. J. Cowling, P. Gai, B. Heinrich, B. Donnio, D. Guillon and J. W. Goodby, *Adv. Funct. Mater*., **2011**, *21*, 1260.
26. M. C. Daniel, J. Ruiz, S. Nlate, J. C. Blais and D. Astruc, *J. Am. Chem. Soc*., **2003**, *125*, 2617.
27. D. V. Leff, P.C. Ohara, J. R. Heath and W. M. Gelbart, *J. Phys. Chem*., **1995**, *99*, 7036.
28. L. Cseh and G.H. Mehl, *Rev. Roum. Chim.*, **2013**, *58*, 879-885.
29. M. Brust, M. Walker, D. Bethell, D. J. Schiffrin and R. Whyman, *Chem. Commun.*, **1994**, 801-802.